Journal of Engineering Science and Technology
Vol. 14, No. 6 (2019) 3105 - 3113

HYDROTHERMAL SYNTHESIS METHOD FOR THE PRODUCTION OF NANOROD TUNGSTEN TRIOXIDE PARTICLES

ASEP BAYU DANI NANDIYANTO*

Departemen Kimia, Universitas Pendidikan Indonesia,
Jl. Dr. Setiabudi No. 229, Bandung 40154, Indonesia
*Corresponding Author: nandiyanto@upi.edu

Abstract

The objective of this study was to demonstrate a hydrothermal synthesis route for the production of nanorod tungsten trioxide (WO_3) particles. The experimental method was done by diluting ammonium tungsten trioxide (ATP; as a model of tungsten raw material) in an aqueous solution and heating it using the hydrothermal process at about 6 bar and 130 °C. To ensure the particle formation mechanism, the processing method was conducted under an additive-free process. Experimental results showed that control of the length and diameter of rod particles can be obtained by adjusting the processing time. The longer processing time gave better conversion of ATP into WO_3 and more growth process of WO_3 to form nanorod, confirmed by the electron microscope and powder crystal analysis. The final particles are still in the amorphous phase since the processing was done at less than 200 °C, informing that this temperature is not sufficient for WO_3 crystallization. This is in a good agreement with thermal decomposition analysis of ATP, replying the need for additional heat treatment to increase the crystallinity of the product. This study gives ideas for further innovations in the hydrothermal synthesis for material production.

Keywords: Hydrothermal, Nanorod, Thermal decomposition, Tungsten trioxide.

1. Introduction

Tungsten trioxide (WO_3) is one of the attractive materials because this material has excellent performance [1, 2]. Especially, this material has an ability to transferring energy from visible light that can be used for solar-related applications such as photocatalysts [3-5].

Many methods have been reported for the production of WO_3 particles. Most of the processes used the heat decomposition route and the acid-basic reaction [6]. To support the production of WO_3, many apparatuses have been suggested, such as spray-assisted fabrication method [7] and hydrothermal process [8-16]. Although the current processes are different, the main idea in the production of WO_3 is almost the same, involving the heating process for interacting tungstate raw components. In general, to prepare WO_3 particles, most of the processes used ammonium tungstate raw material. This type of raw material was used due to its simplification in the decomposition process.

Here, the present report demonstrated the hydrothermal synthesis method for the production of WO_3 particles with controllable morphologies. Hydrothermal was selected due to its simplification process. Further, the simple design of the hydrothermal apparatus makes the process applicable for home-made industry. The present method also used a conventional hydrothermal processing system that can be applied in the close-reaction process. No material in and/or out the system during the conversion of raw material is needed. Although the hydrothermal process for the production of WO_3 has been reported [8-16], there is no information in detail on what mechanism occurring during the conversion process.

Different from other reports, the present study used tungstate raw materials without additional additive or surfactant. This condition can result in the precise analysis for understanding what particle formation mechanism happens during the synthesis process. No porous structure can be produced, while this porous structure can make the unpredictable particle formation mechanism.

Similar to the common process in the WO_3 synthesis route, the present method used ammonium tungstate raw materials. Nandiyanto et al. [6] reported that actually, the three types of commercial ammonium tungstate raw material are available: (i) ammonium normal tungstate ($(NH_4)_2WO_4$), ammonium paratungstate ($(NH_4)_{10}[W_{12}O_{41}]$. m H_2O (m = 4, 5, 7, 10)); and ammonium metatungstate ($(NH_4)_6[W_{12}O_{41}]$. n H_2O (n =1–22)).

Among these types of tungstate raw materials, ammonium paratungstate is the most popular to be used in the production of tungsten-related material. This is because this material has relatively less stability in water, making it easily controlled and handling. Further, it can be controlled to produce high-purity tungsten-related materials and has been applied for various products such as tungstic acid, tungsten metal powder, tungsten carbide, and tungsten oxide. For this reason, as a model of WO_3 raw material, this report used ammonium paratungstate (ATP).

Based on the literature, ATP is easily converted into WO_3 even using direct heat treatment (see Fig. 1). The conversion of ATP into WO_3 was also free of byproduct since the results of ATP decomposition are only water and ammonia gases.

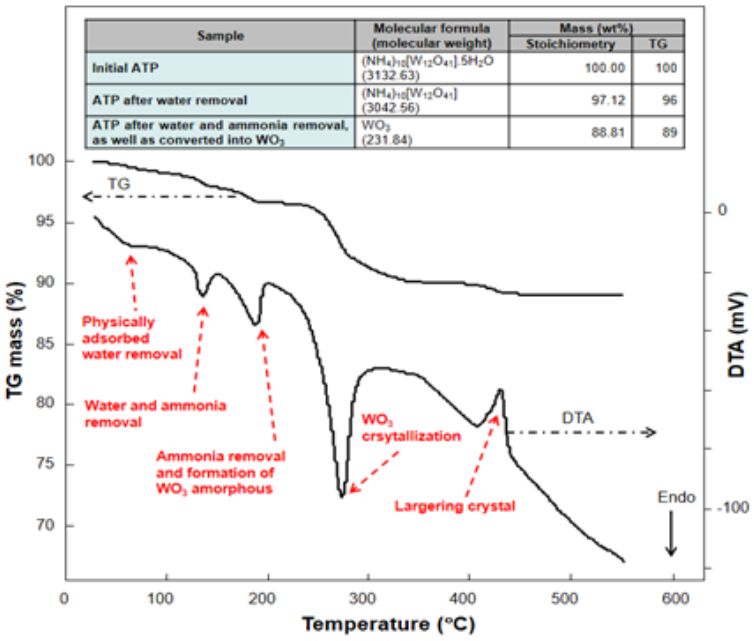

Fig. 1. Thermal analysis of ATP heated at various temperatures [6].

In short, based on literature by Nandiyanto et al. [6, 17, 18], the thermal decomposition of ATP into WO_3 happens into several steps:

Step 1

Water removal process from hydrate components in the ATP. This step was done at temperatures of below 150 °C. The reaction can be written as:

$(NH_4)_{10}[W_{12}O_{41}]. 5\ H_2O \rightarrow (NH_4)_{10}[W_{12}O_{41}] + 5\ H_2O.$

Step 2

Water and ammonia removal process from the ammonium tungstate structure. This step occurs at temperatures of between 150 and 250 °C. This temperature range also allows the formation of WO_3 material with amorphous phase. The reaction can be written as:

$(NH_4)_{10}[W_{12}O_{41}] \rightarrow 12\ WO_3 + 10\ NH_3 + H_2O.$

Step 3

Amorphous to crystal phase transformation. This step happens at temperatures of between 250 and 400 °C.

Step 4

WO_3 crystal growth. This step is done at temperatures of higher than 400 °C.

Finally, the total decomposition of ATP can be explained simply in the following reaction:

$(NH_4)_{10}[W_{12}O_{41}]. 5\ H_2O \rightarrow 12\ WO_3 + 10\ H_2O + 10\ NH_3.$

In the present experimental procedure, ATP was diluted in aqueous solution and heated using a hydrothermal process at about 6 bar and 130 °C. The results showed that control of the length and diameter of rod particles can be obtained by adjusting the processing time.

The longer processing time brought better conversion of ATP into WO_3 and more growth process of WO_3 to form nanorod, confirmed by the Scanning Electron Microscope (SEM) and powder X-Ray Diffraction (XRD) crystal analysis.

In addition, the present reports are found the possible control of particle morphology. This brings good information for further innovations in the synthesis for WO_3 material since the control of morphology bring direct impacts on the material performance, which has been well-documented in the previous report [5-7, 17-21].

2. Method

2.1. Raw chemicals

Nanorod WO_3 particles were prepared from ATP powder (>99%; Kanto Chemical Co., Inc., Japan) and cetyltrimethyl ammonium bromide (CTAB; Sigma Aldrich, US). All chemicals were purchased and used without further purification process.

2.2. Synthesis of particles

Nanorod WO_3 particles were prepared by diluting 1.5 g of ATP and 0.4 g of CTAB in 30 mL of an aqueous solution. The diluted ATP was then put into a 50 mL hydrothermal apparatus and heated at 130 °C using an electrical furnace. The pressure during the hydrothermal process at 130 °C is approximated to be 6 bar. The hydrothermal sample was then centrifuged three times at 4,000 rpm at 5 minutes and rewashed with water. The centrifuged sample was dried at 70 °C to remove water and form a white powder.

2.3. Characterizations

To analyse the prepared particles, the prepared samples were characterized by two characterization methods. One was using XRD (PANalytical X'Pert PRO; Philips Corp., The Netherland), in which, was to analyse the chemical composition and the crystal phase/pattern). The other used a SEM (JSM-6360LA; JEOL Ltd., Japan) that was to characterize the particle outer diameter and morphology.

To analyse the particle size, Feret analysis of the 200 particles were used. Nandiyanto et al. [22] mentioned that detailed information for the Feret analysis is shown in the previous report.

3. Results and Discussion

To confirm the fundamental reason for explaining the particle formation mechanism during the production of WO_3 in the present study, samples were taken at different processing time for examining the particle morphology and crystal structure. The confirmation of the particle morphology by SEM is shown in Figs.

2(a) and (b), and the feret analysis results from the SEM images to support the measurement of the particle sizes are shown in Fig. 2(c). The powder crystal structure analysed by XRD is presented in Fig. 3.

Figure 2 presents the SEM analysis images of ATP hydrothermally at various reaction hours. Different particle morphologies and material crystallinities were obtained, in which, the results were depending on the reaction hours.

Figures 2(a) and (b) show the SEM image analysis results for ATP hydrothermally at 8 and 28 hours of reaction, respectively. The particles were roughly spherical in the initial process (SEM not displayed). The particle shapes are transformed by increasing reaction time. The nanorod particles were obtained after 8 hours of reaction (Fig. 2(a)). Then, the thicker and longer nanorod was obtained with a longer reaction time (Fig. 2(b)).

Control of nanorod length and diameter can be obtained, in which, this can be done by changing the reaction time. The results found that the longer reaction time allowed the formation of the longer and thicker nanorod, confirmed by the high-magnified SEM images shown in the bottom-left image in Figs. 2(a) and (b).

To confirm the possible control in the nanorod length and diameter, detailed information for the correlation between particle length/diameter and reaction time is shown in Fig. 2(c). The results showed that by adding the reaction hours of up to 28 hours, the mean length can be controlled from 0 to about 70 μm, whereas the mean rod diameter can be from 0 to 9 μm.

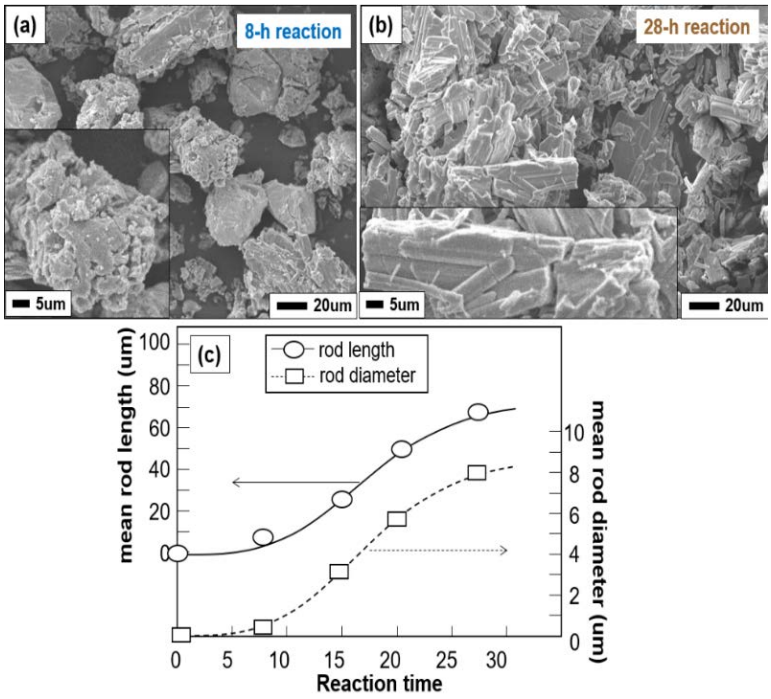

Fig. 2. SEM analysis results of WO_3 nanorod prepared at various reaction time: (a) and (b) are samples taken at 8 and 28 hours of reaction, (c) detailed correlation of rod length/diameter and reaction time.

XRD analysis in Fig. 3 confirmed the transformation of the crystal structure of the particles. The results were compared to the joint committee of powder diffraction system (JCPDS) for WO_3. The standard JCPDS used was JCPDS no. 72-1465 for monoclinic and 75-2187 for hexagonal structure. The XRD result was also compared with the XRD structure for ATP based on studies by Nandiyanto et al. [6, 17, 18]. Initial sample (prior to dilution process) was identical to XRD structure of ATP, and longer reaction time resulted in the transformation of ATP into WO_3 amorphous phase.

At 8 hours of reaction, the ATP structure was still obtained. The amorphous structure was started to be formed. Calculating the area of amorphous and crystal formed resulted that the sample had about 30% of amorphous structure.

The ATP structure disappeared after 10 hours of reaction, informing the process with 10 hours of reaction is the starting time for converting all ATP molecules into WO_3.

The 28-h reaction showed that all ATP structures disappeared. However, it still had particles with an amorphous form.

Although the 28-h reaction had shown the potential production of nanorod (as presented by the SEM image in Fig. 2(b), XRD (presented in Fig. 3) showed that the nanorod has an amorphous phase. According to Nandiyanto et al. [4, 6, 18], the insufficient reaction temperature for crystallizing WO_3 is the main fundamental reason, in which, this is in a good agreement with the thermal decomposition process of ATP in the literature. The literature is shown in Fig. 1 also confirmed that the processing with a temperature of less than 200 °C has successfully converted ATP into WO_3 only without changing the crystal structure.

This result confirmed that the process can allow the production of amorphous WO_3. However, to increase the crystallinity of the product, additional heat treatments, such as heating at a temperature of higher than 300 °C, are required.

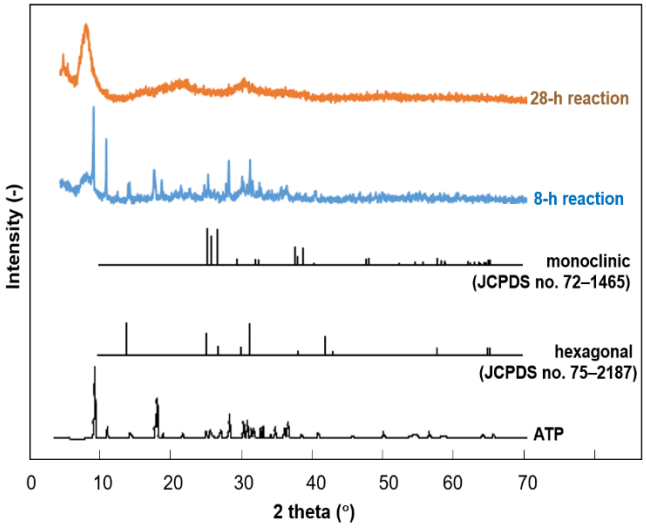

Fig. 3. XRD analysis results of WO_3 nanorod prepared at various reaction hours compared with standard analysis results.

Based on the above results, the possible mechanism for the hydrothermal growth of WO_3 nanostructures is described in Fig. 4. Two types of morphologies were shown. One is a smaller and spherical particle (in the left side of Fig. 4), and the other is a rod particle (in the right side of Fig. 4). A detailed explanation of the mechanism is presented in the following.

In a neutral or weakly basic solution, the starting raw material (i.e., ATP) dissolves as a smaller extent of ammonium tungstate and some parts exist in the form of a single ionic molecule or in a form of a complex of tungsten hydroxide ($W(OH)_x^{m+}$). The dissolution is also helped by the physicochemical properties of ATP that has 5 hydrate component.

Additional heat allows dissolved ATP molecules to bond each other, forming single ionic molecule and complex. Then, the single unit molecule and complex grow to form a tungsten-related crystal. Under ideal condition, the single unit can be grown as a spherical particle.

In the specific condition such as hydrothermal process, these units are then easy to incorporate on the positive (0 0 0 1) and negative (0 0 0 –1) faces of the crystal due to dipole interaction. These faces grow at a faster rate, while the other faces grow slowly. These faces grow and develop larger particles in the final product. The faster-growing faces (see solid red arrows in Fig. 4) become the length of the rod, whereas the other faces (see dashed blue arrows in Fig. 4) are the diameter.

As a consequence, after 28 hours of reaction, larger WO_3 with rod shape can be obtained. This can be found in the SEM result in Fig. 2(b). During the particle growth, the polar face (containing OH component) disappears in the final stage, making the final WO_3 particles precipitated. In addition, to make the WO_3 particles grow, the main component consumed are the single ionic molecule and the simple complex of tungsten hydroxide. Then, these consumption phenomena lower the concentration of single-molecule and simple complex of tungsten hydroxide, resulting the smaller extent of ammonium tungstate to be converted into single-molecule and simple complex components that can be used for the further growth process. This is the main reason for the decreases in the crystal structure of ATP along with the processing time (see XRD results in Fig. 3). ATP converted gradually during the hydrothermal process. And, after 10 hours of reaction, all ATP crystal structures disappeared.

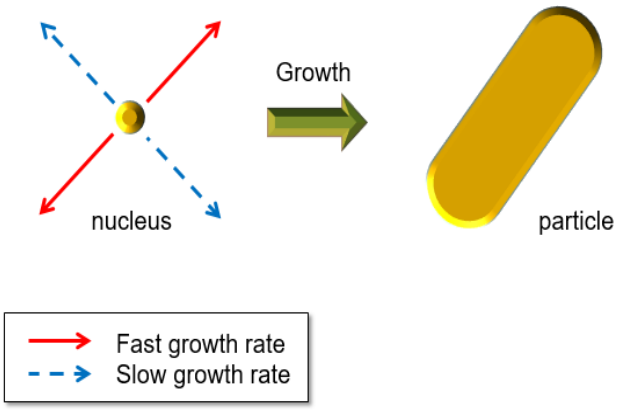

Fig. 4. Illustration mechanism for particle growth.

4. Conclusion

We have demonstrated the successful formation of nanorod WO_3 particles using the hydrothermal synthesis method. The particles were produced by diluting ATP in the aqueous solution and hydrothermally the diluted ATP at about 6 bar and 130 °C. Control of the length and diameter of rod particles can be obtained by adjusting the processing time. The final particles are still in the amorphous phase since the processing was done at less than 200 °C, informing additional treatments for gaining high crystalline WO_3 material. This study brings ideas for further innovations in the hydrothermal synthesis for material production.

Acknowledgements

RISTEK DIKTI (grant-in-aid Penelitian Terapan Unggulan Perguruan Tinggi (PTUPT), Penelitian Terapan (PT), and World-Class Researcher (WCR)) is acknowledged.

References

1. Sudhakaran, R.; Murugan, V.V.; and Sivasakthivel, P.S. (2012). Optimization of process parameters to minimize angular distortion in gas tungsten arc welded stainless steel 202 grade plates using particle swarm optimization. *Journal of Engineering Science and Technology* (*JESTEC*), 7(2), 195-208.
2. Purushotham, E.; and Krishna, N.G. (2014). Synthesis and characterization of tungsten (w) nano particles. *Journal of Engineering Science and Technology Review*, 7(1), 41-44.
3. Buch, V.R.; Chawla, A.K.; and Rawal, S.K. (2016). Review on electrochromic property for WO_3 thin films using different deposition techniques. *Materials Today: Proceedings*, 3(6), 1429-1437.
4. Nandiyanto, A.B.D.; Sofiani, D.; Permatasari, N.; Sucahya, T.N.; Wiryani, A.S.; Purnamasari, A.; Rusli, A.; and Prima, E.C. (2016). Photodecomposition profile of organic material during the partial solar eclipse of 9 March 2016 and its correlation with organic material concentration and photocatalyst amount. *Indonesian Journal of Science and Technology*, 1(2), 132-155.
5. Nandiyanto, A.; Zaen, R.; Oktiani, R.; and Abdullah, A.G. (2018). Photodecomposition profile of curcumin in the existence of tungsten trioxide particles. *IOP Conference Series: Materials Science and Engineering*, 306(1), 012002.
6. Nandiyanto, A.B.D.; Zaen, R.; and Oktiani, R. (2017). Correlation between crystallite size and photocatalytic performance of micrometer-sized monoclinic WO_3 particles. *Arabian Journal of Chemistry.* (in press)
7. Nandiyanto, A.B.D.; Arutanti, O.; Ogi, T.; Iskandar, F.; Kim, T.O.; and Okuyama, K. (2013). Synthesis of spherical macroporous WO_3 particles and their high photocatalytic performance. *Chemical Engineering Science*, 101, 523-532.
8. Zhang, J.; Wang, X.L.; Xia, X.H.; Gu, C.D.; and Tu, J.P. (2011). Electrochromic behavior of WO_3 nanotree films prepared by hydrothermal oxidation. *Solar Energy Materials and Solar Cells*, 95(8), 2107-2112.

9. Su, X.; Xiao, F.; Li, Y.; Jian, J.; Sun, Q.; and Wang, J. (2010). Synthesis of uniform WO_3 square nanoplates via an organic acid-assisted hydrothermal process. *Materials Letters*, 64(10), 1232-1234.
10. Song, X.C.; Zheng, Y.F.; Yang, E.; and Wang, Y. (2007). Large-scale hydrothermal synthesis of WO_3 nanowires in the presence of K_2SO_4. *Materials Letters*, 61(18), 3904-3908.
11. Leghari, S.A.K.; Sajjad, S.; Chen, F.; and Zhang, J. (2011). WO_3/TiO_2 composite with morphology change via hydrothermal template-free route as an efficient visible light photocatalyst. *Chemical Engineering Journal*, 166(3), 906-915.
12. Lee, C.-Y.; Kim, S.-J.; Hwang, I.-S.; and Lee, J.-H. (2009). Glucose-mediated hydrothermal synthesis and gas sensing characteristics of WO_3 hollow microspheres. *Sensors and Actuators B: Chemical*, 142(1), 236-242.
13. Jiao, Z.; Sun, X.W.; Wang, J.; Ke, L.; and Demir, H.V. (2010). Hydrothermally grown nanostructured WO_3 films and their electrochromic characteristics. *Journal of Physics D: Applied Physics*, 43(28), 285501.
14. Ha, J.-H.; Muralidharan, P.; and Kim, D.K. (2009). Hydrothermal synthesis and characterization of self-assembled h-WO_3 nanowires/nanorods using EDTA salts. *Journal of Alloys and Compounds*, 475(1-2), 446-451.
15. Gui, M.-S.; Zhang, W.-D.; Chang, Y.-Q.; and Yu, Y.-X. (2012). One-step hydrothermal preparation strategy for nanostructured WO_3/Bi_2WO_6 heterojunction with high visible light photocatalytic activity. *Chemical Engineering Journal*, 197, 283-288.
16. Chang, K.-H.; Hu, C.-C.; Huang, C.-M.; Liu, Y.-L.; and Chang, C.-I. (2011). Microwave-assisted hydrothermal synthesis of crystalline WO_3–WO_3 0.5 H_2O mixtures for pseudocapacitors of the asymmetric type. *Journal of Power Sources*, 196(4), 2387-2392.
17. Nandiyanto, A.B.D.; Munawaroh, H.S.H.; Kurniawan, T.; and Mudzakir, A. (2016). Influences of temperature on the conversion of ammonium tungstate pentahydrate to tungsten oxide particles with controllable sizes, crystallinities, and physical properties. *Indonesian Journal of Chemistry*, 16(2), 124-129.
18. Nandiyanto, A.B.D.; Oktiani, R.; Ragadhita, R.; Sukmafitri, A.; and Zaen, R. Amorphous content on the photocatalytic performance of micrometer-sized tungsten trioxide particles. *Arabian Journal of Chemistry*. (in press)
19. Arutanti, O.; Ogi, T.; Nandiyanto, A.B.D.; Iskandar, F.; and Okuyama, K. (2014). Controllable crystallite and particle sizes of WO_3 particles prepared by a spray-pyrolysis method and their photocatalytic activity. *AIChE Journal*, 60(1), 41-49.
20. Arutanti, O.; Nandiyanto, A.B.D.; Ogi, T.; Iskandar, F.; Kim, T.O.; and Okuyama, K. (2014). Synthesis of composite WO_3/TiO_2 nanoparticles by flame-assisted spray pyrolysis and their photocatalytic activity. *Journal of Alloys and Compounds*, 591, 121-126.
21. Arutanti, O.; Nandiyanto, A.B.D.; Ogi, T.; Kim, T.O.; and Okuyama, K. (2015). Influences of porous structurization and pt addition on the improvement of photocatalytic performance of WO_3 particles. *ACS Applied Materials and Interfaces*, 7(5), 3009-3017.
22. Nandiyanto, A.B.D.; He, X.; and Wang, W.-N. (2019). Colloid-assisted growth of metal-organic framework nanoparticles. *CrystEngComm*, 14, 2268-2272.